Theory and Simulations of Adhesion Receptor Dimerization on Membrane Surfaces

Yinghao Wu,[†‡§] Barry Honig,[†‡§*] and Avinoam Ben-Shaul[¶*]
[†]Howard Hughes Medical Institute, [‡]Department of Biochemistry and Molecular Biophysics, and [§]Center for Computational Biology and Bioinformatics, Columbia University, New York, New York; and [¶]Institute of Chemistry and the Fritz Haber Research Center, The Hebrew University Safra Campus, Jerusalem, Israel

ABSTRACT The equilibrium constants of *trans* and *cis* dimerization of membrane bound (2D) and freely moving (3D) adhesion receptors are expressed and compared using elementary statistical-thermodynamics. Both processes are mediated by the binding of extracellular subdomains whose range of motion in the 2D environment is reduced upon dimerization, defining a thin reaction shell where dimer formation and dissociation take place. We show that the ratio between the 2D and 3D equilibrium constants can be expressed as a product of individual factors describing, respectively, the spatial ranges of motions of the adhesive domains, and their rotational freedom within the reaction shell. The results predicted by the theory are compared to those obtained from a novel, to our knowledge, dynamical simulations methodology, whereby pairs of receptors perform realistic translational, internal, and rotational motions in 2D and 3D. We use cadherins as our model system. The theory and simulations explain how the strength of *cis* and *trans* interactions of adhesive receptors are affected both by their presence in the constrained intermembrane space and by the 2D environment of membrane surfaces. Our work provides fundamental insights as to the mechanism of lateral clustering of adhesion receptors after cell-cell contact and, more generally, to the formation of lateral microclusters of proteins on cell surfaces.

INTRODUCTION

The three-dimensional structures of the extracellular domains of many adhesion receptors have been determined in atomic detail (1–6), thus enabling a detailed description of the molecular basis of crucial events in cell-cell adhesion. However, there have been only limited theoretical and computational atomic-level studies of protein-protein interactions on membrane surfaces, in part due to the complexity of the systems involved. Adhesion receptors translate and rotate in the two-dimensional (2D) environment of a cell surface and can interact in *cis* with molecules on the same surface and in *trans* with molecules on apposed cell surfaces. In addition, many adhesion processes involve the clustering of proteins into complex supramolecular assemblies (7–10), a phenomenon that is not normally treated by standard molecular simulations.

Given the significant extent of structural characterization of adhesion receptors and their assemblies, a complementary development in theoretical and simulation methodologies can play an important role in the understanding of cell-cell adhesion processes. While there have been numerous studies of protein-protein interactions in three-dimensional (3D) solution, the physical and energetic constraints introduced by the confined 2D environment on membrane-bound proteins are far less understood (11). We recently reported a heuristic theory (12) relating K_d values measured in 3D solution ($K_d^{(3D)}$) to those appropriate to the 2D environment of a membrane surface ($K_d^{(2D)}$). The crucial parameters of the theory depend on structural properties of the protein, specifically the motion of the binding site with respect to the intermembrane normal axis and the rotational freedom of the binding domains. These variables can be obtained from simulations of individual molecules, as was done for monomers and *cis* and *trans* dimers of E- and N-cadherin (12).

In this work, we present a rigorous statistical thermodynamic expression for the ratio $K_d^{(2D)}/K_d^{(3D)}$, and carefully define the molecular and intercellular parameters that relate the two K_d values. The factors that determine *trans* and *cis* binding affinities are discussed in detail and are shown to include spatial and angular factors that have a clear physical meaning. Inherent to the theory are a number of simplifying approximations. To both validate the theory and as a step toward providing a detailed description of adhesion processes, we present a new, to our knowledge, simulation methodology that specifically calculates binding free energies for receptor dimerization in 3D and 2D environments. The very good agreement between the ratios of K_d values obtained from the theory (utilizing simulations of individual molecules) and those derived from direct simulations of the dimerization process between interacting mobile receptors indicates that our approach is robust, and that it can be used to describe essential features of *cis* and *trans* dimerization processes on cell surfaces.

Based on our results we discuss how dimerization affinities are affected by molecular structure, flexibility, and the

Submitted October 14, 2012, and accepted for publication February 7, 2013.

*Correspondence: bh6@columbia.edu or abs@fh.huji.ac.il

Yinghao Wu's present address is Department of Systems and Computational Biology, Albert Einstein College of Medicine, 1301 Morris Park Avenue, New York, NY 10461.

Editor: Lewis Romer.

0006-3495/13/03/1221/9 $2.00

http://dx.doi.org/10.1016/j.bpj.2013.02.009

proximity of the interacting domains to the membrane surface, and comment on the role of membrane elasticity. Further, our work provides estimates of *cis* and *trans* $K_d^{(2D)}$ values for molecules with different $K_d^{(3D)}$ values and different structural and dynamic properties, thus offering a basis for the structure-based interpretation of experimental observations on association/dissociation phenomena on membrane surfaces. Finally, the novel, to our knowledge, simulation methodology we introduce can be applied to cell-surface receptors other than cadherins (13) — the specific focus of this article. We note in this regard that cadherins assemble into ordered structures (adherens junctions) in the complete absence of cytoplasmic interactions in a cooperative process involving both extracellular *trans* and *cis* interactions (2,9,12,13). However, cadherin function, as well as that of essentially all cell-surface molecules, involves interactions with other proteins, both inside and outside the cell, that are influenced by the restrictions arising from the quasi-2D environment provided by a membrane surface. For this reason, we believe that the methods and concepts introduced in this work are of quite general applicability.

THEORY

In this section, we outline the basic statistical thermodynamic treatment that relates the equilibrium constants of the dissociation-association reaction

$$AB \rightleftarrows A + B \tag{1}$$

between membrane bound receptors (Fig. 1), and the corresponding reaction in bulk 3D solution (details can be found in the Supporting Material). We focus primarily on the formation of *trans* dimers but will extend the treatment to *cis* interactions as well. Receptor adhesion in *trans* is mediated by the interaction between two subdomains (labeled *a* and *b* in Fig. 1). In the case of cadherins, these adhesive subdomains are located at the outermost (EC1) repeats of the receptors' ectodomains, and the binding is mediated by the swapping of the two N-terminal β-strands of *a* and *b* (2,13). In Fig. 1, for the sake of simplicity, the ectodomains are depicted as stems with the *trans* binding units at their tips. *Cis* dimerization is mediated by a second interface (schematically illustrated by the *double arrows* in Fig. 1), which in the case of cadherins involves an interaction between the EC1 repeat of one receptor and the linker region connecting EC2 and EC3 of a second receptor (2,13).

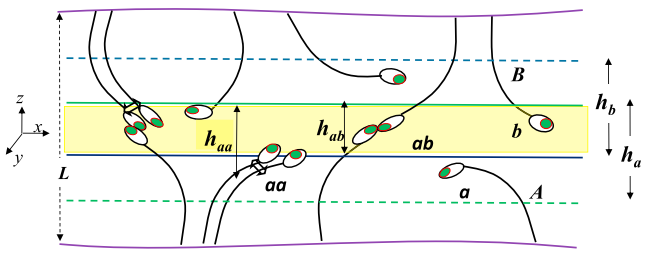

FIGURE 1 Schematic description of the 2D system. Adhesion is mediated by *trans* dimers, bound via their adhesive domains *a* and *b* (*darker dots*) that form the adhesive pair *ab*. Monomers on the same membrane can interact via their *cis* interface *aa* (schematized by *double arrows*). The values h_a, h_b, h_{ab}, and h_{aa} are the ranges of motion along the membrane normal of the corresponding species. (*Highlighted region*) Reaction shell, which is accessible to both *a* and *b*.

Trans dimer formation

Assuming ideal solution behavior, the equilibrium constant of the *trans* binding reaction in the 2D environment is given by

$$K_d^{(2D)} = \frac{\sigma_A \sigma_B}{\sigma_{AB}} = \frac{q_A q_B}{q_{AB}} e^{-\frac{\Delta E_0^{(2D)}}{kT}}, \tag{2}$$

where $\sigma_A = N_A/W$, $\sigma_B = N_B/W$, and $\sigma_{AB} = N_{AB}/W$ are the surface densities of *A* and *B* monomers and *AB* dimers, respectively. The N_I ($I = A, B, AB$) values denote the numbers of molecules in the contact region of area *W*, and q_I is the partition function, per unit area, of a single molecule *I*, calculated using energy levels measured relative to its ground state energy, $E_{0,I}^{(2D)}$ (14). Thus $\Delta E_0^{(2D)} = E_{0,A}^{(2D)} + E_{0,B}^{(2D)} - E_{0,AB}^{(2D)}$ ($\Delta E_0^{(2D)} > 0$) is the dissociation energy of the dimer, where *k* is the Boltzmann's constant, and *T* is the temperature.

Binding free energies ($\Delta G_0 = -kT \ln K_d$) are generally inferred from equilibrium measurements of reaction 1 in bulk 3D solution, whose equilibrium constant is given by

$$K_d^{(3D)} = \frac{\rho_A \rho_B}{\rho_{AB}} = \frac{z_A z_B}{z_{AB}} e^{-\frac{\Delta E_0^{(3D)}}{kT}}. \tag{3}$$

Here $\rho_I = N_I/V$ is the 3D (number) density of $I = A, B, AB$ within the solution volume *V*, and z_I is the molecular partition function of species *I*, per unit volume. We assume that the binding energies in the 2D and 3D environments are equal, because we are considering the same protein-protein interface in both cases, so we set $\Delta E_0^{(2D)} = \Delta E_0^{(3D)} \equiv \Delta E_0$.

The first important factor distinguishing the *trans* binding reaction in 2D from its 3D analog is that *a* and *b*, the adhesive subdomains of *A* and *B*, occupy different, and only partially overlapping, regions of the intermembrane space. As illustrated in Fig. 1, *trans* dimers can only be formed within the reaction shell—the overlap region where both *a* and *b* can be found. More explicitly, if h_a, h_b, and h_{ab} denote, respectively, the ranges of motion of *a*, *b*, and their dimer *ab*, along the membranes' normal (the *z* axis in Fig. 1), then h_{ab} is, by definition, the thickness of the reaction shell. The magnitudes of h_a, h_b, and h_{ab} are dictated by the combined effect of two types of molecular motions: overall rotations of the ectodomain, and internal structural

fluctuations of the ectodomain backbone. Note that only those monomeric receptors whose adhesive subdomains are present within the reaction shell are potentially reactive. In the Supporting Material, we show that this implies

$$K_d^{(2D)} = \frac{h_a h_b}{h_{ab}} \tilde{K}_d^{(3D)}, \quad (4)$$

where $\tilde{K}_d^{(3D)}$ represents the 3D equilibrium constant of the reaction $ab \rightleftarrows a + b$ between the adhesive subdomains in the quasi-3D volume of the reaction shell, $V_{ab} = Wh_{ab}$. That is, $\tilde{K}_d^{(3D)} = (\tilde{\rho}_a \tilde{\rho}_b / \tilde{\rho}_{ab})$, with $\tilde{\rho}_i = \tilde{\sigma}_I / h_{ab}$ denoting the equilibrium 3D densities of a, b, and ab in the reaction shell. We note, however, that $\tilde{K}_d^{(3D)}$ this is not an ordinary 3D constant because the motions, primarily the rotations, of the adhesive subdomains a, b, and ab are constrained by their being connected to the rest of the ectodomain, as opposed to the case of freely rotating receptors in bulk 3D solution. In the Supporting Material, we elaborate on this point and argue that $\tilde{K}_d^{(3D)} / K_d^{(3D)} = (\Delta\omega_a \Delta\omega_b / \Delta\omega_{ab}) / 8\pi^2$, where $K_d^{(3D)}$ is the 3D equilibrium constant in bulk solution and $\Delta\omega_i$ ($i = a, b, ab$) are the rotational ranges of motion (phase space volume) of the binding subdomains of reactive receptors within the reaction shell. For freely rotating receptors in 3D, $\Delta\omega \equiv 8\pi^2$. Substituting this result into Eq. 4, we find that $\lambda = K_d^{(2D)} / K_d^{(3D)}$, the ratio between the 2D and 3D dimerization constants, can be expressed as a product of a spatial factor containing the ranges of motion of a, b, and ab, and a rotational factor involving their angular ranges of motion,

$$\lambda = \frac{K_d^{(2D)}}{K_d^{(3D)}} = \frac{h_a h_b}{h_{ab}} \frac{\Delta\omega_a \Delta\omega_b}{8\pi^2 \Delta\omega_{ab}}, \quad (5)$$

a result that we have previously derived based on heuristic arguments (12), but with $\Delta\omega_i$ calculated for all receptors, whether reactive or not. (In Eq. 5, the $\Delta\omega_i$ values involve only those receptors whose adhesive domains reside within the reaction shell.)

In addition to providing the appropriate conversion unit (i.e., length) between the 2D and 3D constants, we note that (for a given $K_d^{(3D)}$) smaller λ means smaller $K_d^{(2D)}$, and hence enhanced dimerization affinity in 2D. We may thus refer to λ as the equivalent thickness of the reaction shell. Insights into the origin and significance of λ can be gained by further decomposition of Eq. 5 in the form

$$\lambda = L\left(\frac{h_{ab}}{L}\right)\left[\left(\frac{h_a}{h_{ab}}\right)\left(\frac{h_b}{h_{ab}}\right)\right]\left(\frac{\Delta\omega_{ab}}{8\pi^2}\right)\left[\left(\frac{\Delta\omega_a}{\Delta\omega_{ab}}\right)\left(\frac{\Delta\omega_b}{\Delta\omega_{ab}}\right)\right], \quad (6)$$

where all the factors except the first (L, the thickness of the intermembrane gap) are dimensionless. We consider two special cases and then a realistic one:

1. In the limit where the adhesive subdomains of all species (a, b, and ab) can freely translate and rotate anywhere within the entire intermembrane space (so that $h_a = h_b = h_{ab} = L$, and $\Delta\omega_a = \Delta\omega_b = \Delta\omega_{ab} = 8\pi^2$), this volume is equivalent to that of an ordinary 3D solution, and $\lambda = L$ is simply the numerical-dimensional conversion factor relating the 3D and 2D dissociation constants.
2. If all of the adhesive subdomains a, b, and ab are present and can freely rotate (i.e., $\Delta\omega_a = \Delta\omega_b = \Delta\omega_{ab} = 8\pi^2$) and translate (i.e., $h_a = h_b = h_{ab}$) within the same narrow shell, then $\lambda = h_{ab}$ is simply the thickness of the reaction slab, similar to Bell's original model (15,16).
3. Realistically, dimer formation will add restrictions to molecular motions so that, in general, $h_a < h_{ab}$, $h_b < h_{ab}$. Thus, the two spatial factors in the square brackets in Eq. 6 tend to increase the effective thickness of the reaction shell (λ) beyond its physical size (h_{ab}), effectively lowering the dimerization affinity. The qualitative effects of the angular factor on λ are more complicated. In general, due to restricted rotational motion in 2D relative to 3D, $(\Delta\omega_{ab}/8\pi^2) < 1$. On the other hand, restrictions in motion due to dimerization result in $(\Delta\omega_a / \Delta\omega_{ab})(\Delta\omega_b / \Delta\omega_{ab}) > 1$. The combined effect depends on the details of the system involved but in the next section we show that, for the case of cadherins, $\Delta\omega_a \Delta\omega_b / 8\pi^2 \Delta\omega_{ab} < 1$, revealing that the limited rotational freedom of the monomers in the 2D system favors dimer formation.

Cis dimer formation

By a straightforward extension, Eq. 5 can be applied to describe other association processes. Thus, for instance, the ratio between the 2D and 3D equilibrium constants of *cis* dimerization of two receptors of type A, $(AA(cis) \rightleftarrows A + A)$, is obtained by replacing every subscript b by a, yielding (see Fig. 1)

$$\lambda_{cis} = \frac{K_{d,cis}^{(2D)}}{K_{d,cis}^{(3D)}} = \frac{h_a^2}{h_{ab}} \frac{\Delta\omega_a^2}{8\pi^2 \Delta\omega_{aa}}. \quad (7)$$

Analogously, we can extend Eq. 6 to estimate the equilibrium constants corresponding to *cis* dimerization of a monomer and a *trans* dimer, or two *trans* dimers, etc.

SIMULATION METHODOLOGY

Dynamic and individual MC simulations

The Monte Carlo (MC) simulation algorithm described in this section uses realistic structural and dynamical representations of receptor conformations to enable a direct determination of $K_d^{(2D)}$ and $K_d^{(3D)}$ and hence of their ratio, $\lambda = K_d^{(2D)} / K_d^{(3D)}$. We refer to these calculations as dynamical-MC (DMC) simulations. To compare their results to the theoretical predictions of Eq. 5, the h_i and $\Delta\omega_i$ appearing in Eq. 5 are evaluated by separately sampling monomer and dimer configurations from those encountered in

the course of the DMC simulations. This is equivalent to simulating the motion of isolated, translationally immobile yet structurally flexible receptors, yielding similar information to that obtained in our previous work (12). We refer to these calculations as IMC simulations (*I* for individual or isolated receptors).

Deriving 2D and 3D equilibrium constants from simulations

At low densities, the equilibrium concentrations of monomers and dimers can be obtained from DMC simulations of a system containing just two interacting receptors. Fig. 2 outlines our overall approach. Monomers translate, rotate, and undergo structural fluctuations, and upon encounter may form a dimer, which also translates and rotates and eventually dissociates, with probabilities that depend on the binding energy, following the usual Metropolis procedure. The equilibrium concentrations are determined by the relative frequencies of finding the pair of receptors bound or dissociated. Fig. 2 *a* describes the simulations in 3D. At time zero, the monomers are not in contact but occasionally a dimer is formed and the energy of the system decreases by an amount equal to the binding energy. The dimer can then dissociate with a corresponding increase in the energy of the system, and the simulation continues. Fig. 2 *b* shows the same behavior in a constrained 2D environment. Note that the dimerization energy is the same in both cases. The equilibrium constants (and hence the dimerization free energies) are determined by the time intervals, τ_{AB} and τ_{A+B}, which denote the sum of time intervals that the pair of receptors in the simulation box is bound or dissociated, respectively. Provided the total simulation time, $\tau = \tau_{AB}$ and τ_{A+B}, is long enough, then τ_{A+B}/τ is the probability of finding receptors *A* and *B* in their unbound state, and $\tau_{AB}/\tau = 1 - \tau_{A+B}/\tau$ is the probability of finding them dimerized. Specifically, $\rho_A/\rho_{AB} = \rho_\beta/\rho_{AB} = \tau_{A+B}/\tau_{AB}$ and $\sigma_A/\sigma_{AB} = \sigma_\beta/\sigma_{AB} = \tau_{A+B}/\tau_{AB}$, in the 3D and 2D systems, respectively. The Supporting Material includes a movie describing the association of two monomers into a *trans* dimer.

Simulation conditions and parameters

In the 3D system (Fig. 2 *a*) the two receptors were placed in a cubic box of volume $V = L_x L_y L_z = (20\ \text{nm})^3 = 8000\ \text{nm}^3$, with periodic boundary conditions in all directions. The 2D simulation box consists of two parallel membranes of area $W = L_x L_y = (50\ \text{nm})^2 = 2500\ \text{nm}^2$, separated from each other by a distance $L_z \equiv L = 24$ nm (corresponding to one layer of *trans* dimers in the crystalline state (2)), using periodic boundary conditions in the *x* and *y* directions. The two bow-like monomers comprising a *trans* dimer are embedded in different (nearly orthogonal) planes. Their end-to-end vectors are tilted by ~40° relative to the membrane normal. The dimensions of the 2D and 3D boxes are not much larger than the maximal length of a monomer (~20 nm) or a *trans* dimer (~38 nm), yet considerably larger than the dimensions (~4 nm) of the adhesive (EC1) subdomain of cadherins (2).

As in our previous work, a full C_α representation is used to model the structure and conformational dynamics of the cadherin receptors. Structural fluctuations (such as bending or twisting) around the average structure of the cadherin ectodomain are accounted for by the normal mode motions (17–19) of the hinge domains that link adjacent EC repeats (12). In addition, and crucially so in the DMC simulations, the receptors are allowed to perform both translational and rotational motions, in both the 3D and 2D systems. In the 2D system, lateral translation of monomers is mediated by EC5 diffusion parallel to the membrane plane. Dimer translation involves concerted movement of the two EC5 ends, allowing for small changes in their relative position and distance, provided they keep the dimer intact. Monomers undergo rotational motions, subject to the assumed flexibility of the EC5 subdomain with respect to the membrane surface. The EC5 domains of the monomers comprising a *trans* dimer are allowed the same range of rotation angles as in their free state; however, due to the additional constraints implied by the binding interface of their EC1 domains, the actual range of their EC5 rotations is far more restricted than those of the free monomers.

In both the 2D and 3D systems, a stable *trans* dimer is defined by the requirement that the root-mean square deviation (RMSD) of the C_α values comprising the pair of EC1(*A*)-EC1(*B*) domains is <6 Å, with respect to the known crystal structure. This criterion was established based on MD simulations of individual *trans* dimers as discussed previously in Wu et al. (12). When this condition is met, the dimer is assigned the binding energy ΔE_0. Two- and three-dimensional simulations were carried out for ΔE_0 between 5 and 10 *kT* at 1 *kT* intervals. In the 3D simulations, the two monomers perform independent movements, consisting of a sequence of random translational moves, followed by random rotations, and internal conformational changes. If the centers of mass of EC1(*A*) and EC1(*B*) happen to be close to each other (specifically, <50 Å apart), the RMSD of the EC1(*A*)-EC1(*B*) pair is calculated and if it is less than the 6 Å cutoff, a *trans* dimer is assumed to form, stabilized by ΔE_0. Otherwise, the monomers continue their random motions. Once a dimer is formed, it is also allowed to translate and rotate, as well as to undergo internal conformational changes of its constituent monomers. If the independent conformational changes of the monomers result in an RMSD of the EC1(*A*)-EC1(*B*) pair larger than 6 Å, i.e., a dissociated dimer, the move is accepted with the Metropolis probability $\exp(-\Delta E_0/kT)$, and so on (20). The same procedure is used in the 2D simulations, augmented by the restrictions on EC5 motion. Separate 2D simulations were carried out for five different values of $\Delta\Omega = \Delta(\cos\Theta)\Delta\Phi\Delta\Psi$, the range of angular motion of the membrane-anchored subdomain (EC5), and hence also of the entire ectodomain. Specifically, $\Delta\Theta$ is used to define the range of polar angles available to the long axis of EC5 around its equilibrium (crystal structure) orientation ($\Theta_0 \approx 20°$) relative to the *z* axis. The angle Φ is between the projection of the EC5 axis on the *x*,*y* (membrane) plane and the *x* axis, and Ψ is the angle of rotation of EC5 around its own long axis (resulting in rotation of the plane containing the bow-like ectodomain). The azimuthal angle of the membrane bound receptors is not restricted, so that $0 \le \Phi \le 2\pi$. Larger $\Delta\Omega$ values imply larger values of all the h_i values (h_a and h_b are always larger than h_{ab}). Note, however, that significant contributions to all h_i values arise also from structural fluctuations associated with normal mode vibrations in the linker regions between adjacent EC repeats. Thus, the h_i values are nonzero even when no EC5 rotations are allowed ($\Delta\Theta = \Delta\Psi = 0°$). Simulations

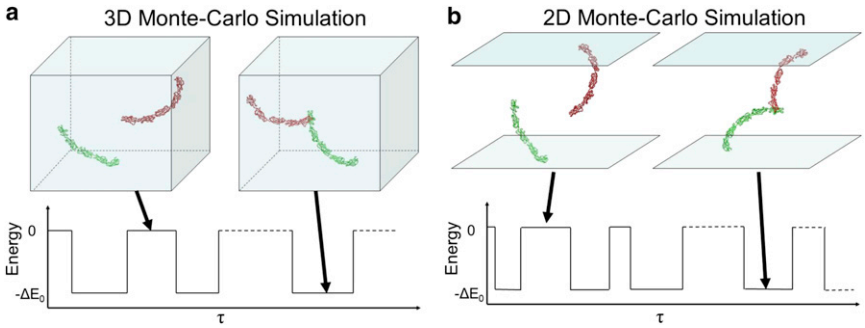

FIGURE 2 Schematic illustration of the simulation boxes used to calculate *trans* dimer binding affinities of freely translating and rotating receptors in 3D (*a*) and 2D (*b*). (*Lower traces*) Temporal fluctuations determining the dynamical equilibrium between monomer and dimer states; τ is the simulation time.

were carried out for five different values of $\Delta\Omega$; that is, $\Delta\Theta = \Delta\Psi = 0°$, 5°, 10°, 30°, and 60°, with no restrictions on Φ. EC5 orientations were uniformly sampled within the specified ranges of Θ and Ψ, discarding conformations which cross the membrane surface.

RESULTS

We carried out DMC simulations of $K_d^{(3D)}$ and $K_d^{(2D)}$ that correspond to cadherin *trans* dimerization, for several different choices of the binding energies (ΔE_0), and different extents of angular flexibility of the membrane bound receptors ($\Delta\Omega$, as defined above). For each case, we calculated the ratio $\lambda = K_d^{(2D)}/K_d^{(3D)}$ obtained from the DMC simulations, and compared it to the theoretical value derived from Eq. 5, with molecular parameters evaluated using IMC simulations. Because λ has a nanometer scale, we find it convenient to express the surface (2D) concentrations, σ, and thus $K_d^{(2D)}$, in units of nm^{-2} (i.e., molecules/nm^2) or μm^{-2}, and the 3D concentrations, ρ, and correspondingly $K_d^{(3D)}$, in units of nm^{-3} or μm^{-3}. Note that the relationship between $K_d^{(3D)}$ and the corresponding constant in molar units, $K_{d,C}^{(3D)}$, follows simply from the identity 1 nm^{-3} = 10^9 μm^{-3} = 1.67 M, yielding $K_d^{(3D)} = 1.67K_{d,C}^{(3D)}$ (for $K_d^{(3D)}$ expressed in nm^{-3}) . The corresponding binding free energies, $\Delta G_0^{(3D)} = -kT \ln K_d^{(3D)}$ and $\Delta G_{0,C}^{(3D)} = -kT \ln K_{d,C}^{(3D)}$, differ by $\Delta G_0^{(3D)} = \Delta G_{0,C}^{(3D)} - 0.51\ kT$.

3D dimerization constants and affinities

From the 3D DMC simulations we derived $K_d^{(3D)}(trans)$ for $\Delta E_0 = 5,\ldots,10\ kT$. The corresponding binding free energies, $\Delta G_0^{(3D)}/kT = -\ln K_d^{(3D)}$, are shown in Fig. 3. The linear increase of $\Delta G_0^{(3D)}$ with ΔE_0 (with slope 1) reveals that the entropic component of the binding affinity, $T\Delta S_0^{(3D)} = \Delta E_0 - \Delta G_0^{(3D)} \approx 3.5\ kT$, is a constant, independent of the binding energy. Moreover, $T\Delta S_0^{(3D)} > 0$, indicating that dimer dissociation is favored on entropic grounds. Note that $\Delta S_0^{(3D)}$ (as well as $\Delta S_0^{(2D)}$ below) correspond to entropy changes associated solely with the nontranslational degrees of freedom (i.e., internal vibrations and rotations as well as overall rotations) of the receptors (21) (e.g., Ben-Shaul and Gelbart (22), and see the Supporting Material).

2D dimerization constants and affinities

Binding affinities of membrane bound receptors, $\Delta G_0^{(2D)}/kT = -\ln K_d^{(2D)}$, were derived from DMC simulations for the same six values of ΔE_0 used in the 3D simulations. For every value of ΔE_0, simulations were performed for the abovementioned values of $\Delta\Omega$ ($\Delta\Theta = \Delta\Psi = 0°$, 5°, 10°, 30°, and 60°, with no restriction on Φ). The results are shown in Fig. 4. Although in this case the numerical errors are slightly larger than in Fig. 3, it is again apparent that $\Delta G_0^{(2D)}$ increases linearly with ΔE_0 in all cases considered, and the slope is again 1. Thus, as in 3D, $\Delta S_0^{(2D)}$ is a constant, independent of ΔE_0. We note, however, that $\Delta S_0^{(2D)}$ depends on $\Delta\Omega$: a larger $\Delta\Omega$ implies greater rotational-conformational freedom (hence entropy) of the receptors, which is primarily pronounced in their unbound monomeric state. This increase is somewhat implicit in Fig. 4, but can be clearly seen in Fig. 5, where we note that $\Delta S_0^{(2D)}$ increases from ~2 k to ~4 k as $\Delta\Omega$ increases from 0° to 60°. These values are comparable in magnitude to the 3D entropy change of $\Delta S_0^{(3D)} \approx 3.5\ k$, yet it should be noted that unlike in the 3D system, where the major contribution to $\Delta S_0^{(3D)}$ arises from the overall rotations of the receptors, the major (positive) contribution to $\Delta S_0^{(2D)}$ results from the spatial factor ($\Delta S_{0,sp}^{(2D)} = k \ln[(h_a/h_{ab})(h_b/h_{ab})]$), which has no 3D counterpart. The angular contribution to $\Delta S_0^{(2D)}$ is rather small compared to the 3D case, reflecting the fact that, in general, $\Delta\omega_a\Delta\omega_b/8\pi^2\Delta\omega_{ab} < 1$.

The ratio $K_d^{(2D)}/K_d^{(3D)}$: comparing simulation to theory

In Fig. 6 we show the values obtained for $\lambda = K_d^{(2D)}/K_d^{(3D)}$ from the DMC simulations, and compare them to those predicted by Eq. 5 using spatial and angular ranges of motions obtained from IMC simulations. The agreement between the two approaches is very good. As expected, the results in

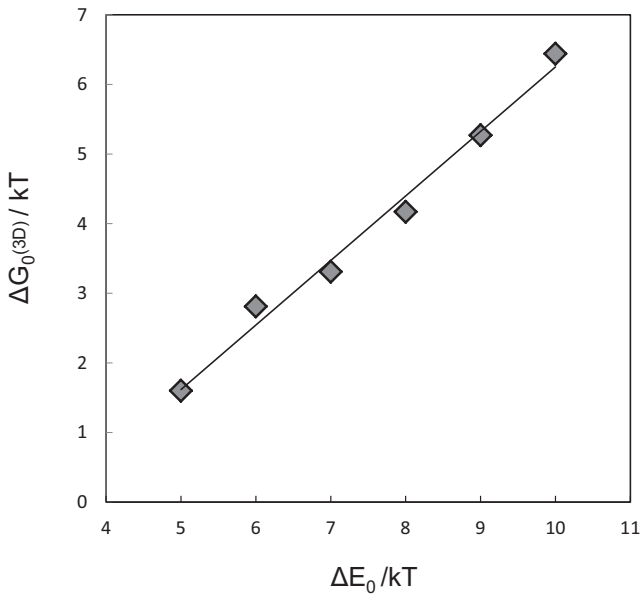

FIGURE 3 The binding free energy in 3D as a function of the adhesion energy. The linear dependence, with unit slope, indicates that $\Delta S_0^{(3D)} = (\Delta E_0 - \Delta G_0^{(3D)})/T \approx 3.5\ k$ is independent of the binding energy.

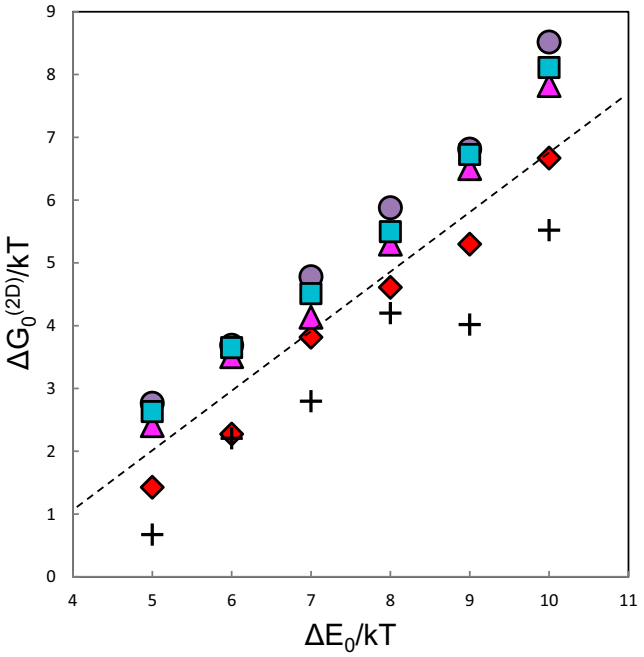

FIGURE 4 The binding free energy of a cadherin *trans* dimer in 2D as a function of the adhesion energy, for five different values of the angular range, $\Delta\Omega$, available to the membrane bound (EC5) subdomain. (Specifically, $\Delta\Omega$ refers to $\Delta\Theta = \Delta\Psi$, while in all cases $\Delta\Phi = 2\pi$.) (*Circles*, *squares*, *triangles*, *diamonds*, *crosses*) $\Delta\Omega = 0°$, 5°, 10°, 30°, and 60°, respectively. (*Straight dashed line*) Guide to the eye. Its slope is 1, indicating that in all five cases the dissociation entropy in reaction 1, $\Delta S_0^{(2D)} = (\Delta E_0 - \Delta G_0^{(2D)})/T$, is independent of the binding energy. As expected, $\Delta S_0^{(2D)}$ increases with $\Delta\Omega$.

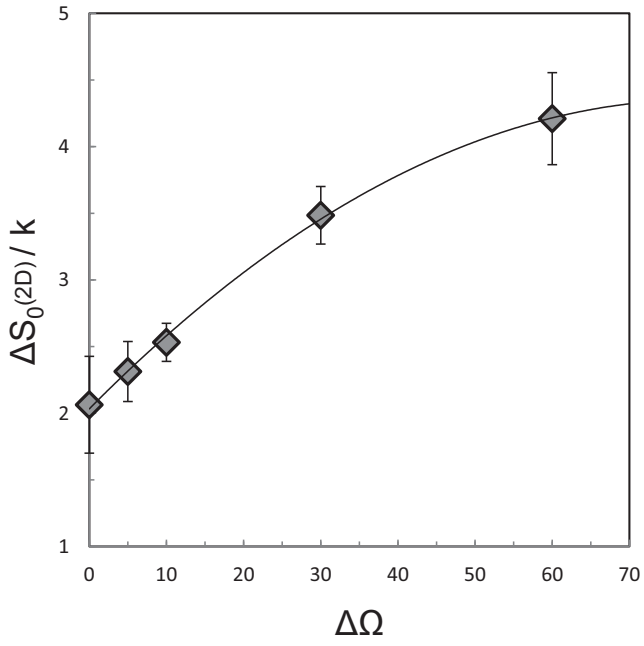

FIGURE 5 The standard 2D entropy change of cadherin dimer dissociation (reaction 1) in 2D, as a function of the angular allowance $\Delta\Omega$ (see legend to Fig. 4).

Fig. 6 reveal that λ gets larger as the flexibility ($\Delta\Omega$) of the receptor's ectodomain increases, and that in all cases it is considerably smaller than the intermembrane distance ($L = 24$ nm). Less obvious is the fact that in all cases considered, λ is still significantly smaller than h_{ab}, indicating that the angular factor in Eq. 6 favors *trans* dimer formation to the extent that it overcompensates the effect of the spatial factor, which disfavors this process. (Specifically, we found $\lambda \approx 0.25$, 0.30, 0.38, 0.99, and 2.17 nm as compared to $h_{ab} \approx 1.5$, 1.5, 2.5, 5.0, and 6.0 nm, for $\Delta\Omega = 0°$, 5°, 10°, 30°, and 60°, respectively.)

DISCUSSION

In the Theory section and in the Supporting Material we presented the basic statistical-thermodynamic principles underlying the formation of *trans* dimers, and outlined the extension of these notions to *cis* interactions between receptors that diffuse on the same membrane. These ideas were then corroborated based on detailed Monte Carlo simulations modeling the *trans* interaction between cadherin receptors. The theory and simulation methodology presented in this work are directly applicable to other membrane-bound receptors. The molecular parameters appearing in Eqs. 5 and 6 can be obtained using our simulation methodology or estimated based on the properties of the particular system of interest. We note, however, that many cell surface receptors are composed of strings of immunoglobulin-like domains and that the results obtained in this work offer first-order approximations of λ for many of these

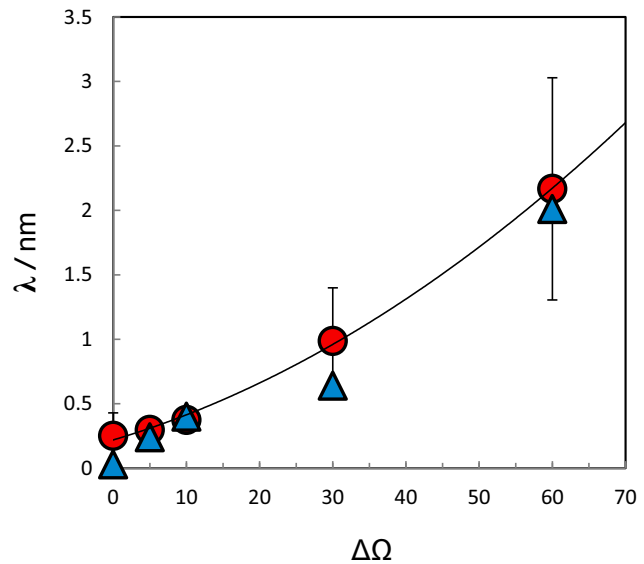

FIGURE 6 The ratio between the equilibrium constants of reaction 1 in the 2D and 3D environment, $\lambda = K_d^{(2D)}/K_d^{(3D)}$, as a function of the angular allowance $\Delta\Omega$. (*Circles*) Results of the dynamic Monte Carlo simulations. (*Triangles*) Results obtained using Eq. 5, with molecular parameters (h_i, $\Delta\omega_i$) derived from the IMC simulations of structural fluctuations of immobile receptors.

proteins. Obviously, the expectation is that λ will increase as the number of extracellular domains increases and as the linkers between them become more flexible. Below we summarize key results of our analysis and discuss factors that are relevant to cell-surface proteins in general.

Relating 2D to 3D *trans* interactions

Equation 5, which represents the ratio between the 2D and 3D dimerization constants as a product of spatial and angular components, offers a clear picture of the factors that determine dimerization affinities in the intercellular space. The subsequent factorization in Eq. 6 provides additional insights into this scheme, as exemplified by the special cases discussed above. Two of the factors in this equation, h_{ab}/L and $\Delta\omega_{ab}/8\pi^2$, which account for the spatial and angular confinements of the adhesive subdomains, are present in all systems. Both of these factors tend to reduce $\lambda = K_d^{(2D)}/K_d^{(3D)}$ and thus favor the adhesion affinity in 2D relative to the 3D environment. On the other hand, the two factors in square brackets in Eq. 6, reflecting the spatial and angular entropy losses upon dimerization, depend more sensitively on the structural-dynamical properties of the adhesive receptors involved. Thus, for example, relatively long and semiflexible receptors such as cadherins are likely to suffer greater entropy losses upon dimerization than shorter and less flexible proteins such as T-cell receptors.

Relating 2D to 3D *cis* interactions

Although this article has focused on *trans* interactions, the same theoretical and qualitative principles come into play when *cis* interaction is involved. One basic difference, of course, is that *cis* interactions do not depend on intermembrane spacing and, in principle, can take place between any two cell surface proteins. It is thus important to estimate the relevant dissociation constants, $K_{d,cis}^{(2D)}$. For the specific case of cadherin monomers, *cis* dimerization affinities are quite weak, $K_{d,cis}^{(3D)} \geq 1$ mM. Using an expression similar to Eq. 7, we showed that this value translates to $K_{d,cis}^{(2D)} \leq 500\ \mu\text{m}^{-2}$, suggesting that cadherins tend not to dimerize in 2D. The weak binding affinity is due in part to the weak *cis* binding energy, but also to the considerable configurational entropy loss of the monomers upon dimerization (see Eq. 7). Notably, however, the *cis* binding affinity increases dramatically when one of the monomers is already engaged in a *trans* dimer, because a substantial portion of the *cis* dimerization entropy penalty has already been paid when the *trans* dimer was formed. The effect is even more pronounced when two *trans* dimers interact in *cis*.

It is also important to consider the possibility that *cis* interactions will occur on their own, even when the 3D affinities are weak. If, for example, unlike in cadherins, the *cis* binding interface is located on membrane proximal domains (23), one expects lower entropy losses upon dimerization because fewer interdomain linkers are rigidified by dimerization. Indeed, using Eq. 7 we estimated the hypothetical *cis* dimerization affinities of two cadherins mediated by either their EC4, EC3, or EC2 interfaces, and found that $K_{d,cis}^{(2D)}$ decreases dramatically, from the value mentioned above of ~500 μm^{-2} for EC1-EC1 mediated dimerization to ~25 μm^{-2} for EC4-EC4 adhesion. The latter case corresponds to a binding affinity of ~9 kT, which is strong enough to induce substantial lateral aggregation (24). We speculate that at least in some cases, glycosylation of membrane proximal domains may play a role in preventing lateral receptor aggregation.

Clustering of adhesion receptors

The formation of intercellular *trans* dimers is often followed by their clustering in cell-cell contact regions (1,25,26). Different theoretical approaches were suggested to account for this phenomenon, including models invoking *cis*/*trans* coupling, segregation of long and short receptors, and membrane fluctuations effects (27–29). In a previous study (24) we presented a lattice model whereby cooperative *cis*/*trans* interactions among cadherin receptors lead to a 2D phase transition resulting in the formation of a condensed 2D junction phase (e.g., an adherens junction), composed (mostly) of *trans* dimers.

We also showed that the formation of ordered junctions is greatly enhanced, especially at low expression levels, through the diffusion trap mechanism (see, e.g., Perez et al. (30)), as schematically illustrated in Fig. 7. In this mechanism, once a stable adhesive region between two cells is nucleated (e.g., after initial contact between two curved cell surfaces or protrusions), it serves as a trap, attracting additional monomers that migrate into this region, thus forming additional *trans* dimers. The dimer binding energy compensates for the reduced translational entropy of the

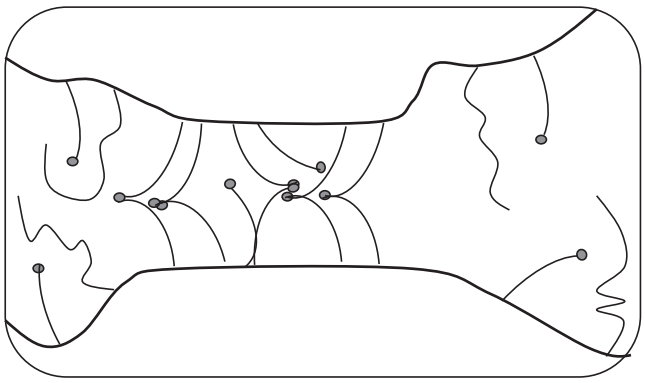

FIGURE 7 Receptor clustering in the diffusion trap. Membrane regions around the contact region can distance from each other if the receptors cluster, thus gaining curvature undulation entropy.

receptors in the crowded trap environment. If long molecules whose size is incompatible with the preferred intermembrane distance were initially present in the contact zone, they can diffuse away from this region, thereby enjoying greater configurational entropy. In addition, membrane regions around the trap can more freely undergo elastic curvature fluctuations, providing an additional potential driving force for receptor clustering (29,31,32).

Molecules such as cadherins and ephrins form ordered junctions in cell-cell contact zones due to well-defined interprotein *cis* interfaces, but it is not clear that this is the general case. In other systems, comparable 2D lattices have yet to be identified, although ordered one-dimensional arrays are frequently observed (1). However, even in the absence of lateral interactions, the diffusion trap mechanism (30) will lead to a buildup of density in the contact zone (33,34). In such cases, the clusters observed experimentally are likely to be disordered (liquid-like) (35), yet much remains to be done before this issue is resolved.

Membrane fluctuations

Our model of the intercell contact region, as consisting of two plane parallel membranes at a fixed distance from each other, is obviously approximate, because it totally ignores the possible effects of fluctuations in intermembrane distance as a result of intrinsic membrane curvature fluctuations or cytoplasmic events that can influence this distance. This picture is applicable to locally flat contact regions where receptor density is relatively high, of the kind associated with the diffusion trap mentioned above. An order-of-magnitude estimate of membrane curvature effects in such regions can be obtained based on the premise that intact *trans* dimers dictate a well-defined intermembrane distance.

The average amplitude of the height fluctuations presented by a membrane undergoing random thermal undulations is given by $\langle u^2\rangle^{1/2} = cl(kT/\kappa)^{1/2}$ (4,30,36), where $c \approx 0.1$ is a dimensionless numerical constant, κ is the bending modulus of the membrane (37), and l^2 is the area of a fluctuating membrane patch whose edges are kept stationary. If *trans* dimers can be regarded as membrane pinning points, then for a typical bending rigidity of a biological cell membranes with, e.g., $\kappa = 400\ kT$ (38), we find, assuming an interreceptor distance of 50 nm (appropriate to relatively high cell surface expression levels), that $\langle u^2\rangle^{1/2} \approx 0.2$ nm. This value is much smaller than the assumed intermembrane separation, $L = 24$ nm, considerably smaller than the ranges of motion of the cadherin monomers (h_a,h_b) and even smaller than the range of motion of the dimer interface (h_{ab}). The actual value of $\langle u^2\rangle^{1/2}$ may be higher, owing to the fact that isolated *trans* dimers are not entirely rigid and may tolerate small changes in the intermembrane distance. In any case, this simple estimate suggests that membrane fluctuations in crowded contact regions are likely to be small. Nevertheless, we note that local membrane fluctuations can be incorporated approximately in the theoretical framework, by adding their contributions to the monomers' ranges of motion (h_a,h_b); their effect on dimer fluctuations is expected to be smaller. However, extensions and ramifications of this kind for specific systems are warranted and instructive only when the dynamical and structural aspects of the relevant adhesive receptors and the membranes to which they are bound are realistically represented.

SUPPORTING MATERIAL

One figure, six equations, and a movie are available at http://www.biophysj.org/biophysj/supplemental/S0006-3495(13)00194-X.

We thank Larry Shapiro and Bill Gelbart for helpful discussions.

The financial support of the US-Israel Binational Science Foundation (grant No. 659/06 to A.B.-S. and B.H.), and the U.S. National Science Foundation (grant No. MCB 0918535 to B.H.) is gratefully acknowledged. A.B.-S. also thanks the Israel Science Foundation (grant No. 1448/10) and the Archie and Marjorie Sherman chair.

REFERENCES

1. Aricescu, A. R., and E. Y. Jones. 2007. Immunoglobulin superfamily cell adhesion molecules: zippers and signals. *Curr. Opin. Cell Biol.* 19:543–550.
2. Harrison, O. J., X. Jin, …, B. Honig. 2011. The extracellular architecture of adherens junctions revealed by crystal structures of type I cadherins. *Structure.* 19:244–256.
3. Seiradake, E., K. Harlos, …, E. Y. Jones. 2010. An extracellular steric seeding mechanism for Eph-ephrin signaling platform assembly. *Nat. Struct. Mol. Biol.* 17:398–402.
4. Springer, T. A. 1990. Adhesion receptors of the immune system. *Nature.* 346:425–434.
5. Rudolph, M. G., R. L. Stanfield, and I. A. Wilson. 2006. How TCRs bind MHCs, peptides, and coreceptors. *In* Annual Review of Immunology. Annual Reviews, Palo Alto, CA. 419–466.
6. Hartman, N. C., and J. T. Groves. 2011. Signaling clusters in the cell membrane. *Curr. Opin. Cell Biol.* 23:370–376.
7. Monks, C. R. F., B. A. Freiberg, …, A. Kupfer. 1998. Three-dimensional segregation of supramolecular activation clusters in T cells. *Nature.* 395:82–86.
8. Kanchanawong, P., G. Shtengel, …, C. M. Waterman. 2010. Nanoscale architecture of integrin-based cell adhesions. *Nature.* 468:580–584.
9. Hong, S., R. B. Troyanovsky, and S. M. Troyanovsky. 2010. Spontaneous assembly and active disassembly balance adherens junction homeostasis. *Proc. Natl. Acad. Sci. USA.* 107:3528–3533.
10. Harris, T. J. C., and U. Tepass. 2010. Adherens junctions: from molecules to morphogenesis. *Nat. Rev. Mol. Cell Biol.* 11:502–514.
11. Dustin, M. L., S. K. Bromley, …, C. Zhu. 2001. Identification of self through two-dimensional chemistry and synapses. *Annu. Rev. Cell Dev. Biol.* 17:133–157.
12. Wu, Y. H., J. Vendome, …, B. Honig. 2011. Transforming binding affinities from three dimensions to two with application to cadherin clustering. *Nature.* 475:510–513.
13. Brasch, J., O. J. Harrison, …, L. Shapiro. 2012. Thinking outside the cell: how cadherins drive adhesion. *Trends Cell Biol.* 22:299–310.
14. Hill, T. L. 1960. Introduction to Statistical Thermodynamics. Addison-Wesley, New York.

15. Bell, G. I. 1978. Models for the specific adhesion of cells to cells. *Science.* 200:618–627.

16. Bell, G. I., M. Dembo, and P. Bongrand. 1984. Cell adhesion. Competition between nonspecific repulsion and specific bonding. *Biophys. J.* 45:1051–1064.

17. Li, G. H., and Q. Cui. 2002. A coarse-grained normal mode approach for macromolecules: an efficient implementation and application to Ca^{2+}-ATPase. *Biophys. J.* 83:2457–2474.

18. Tama, F., F. X. Gadea, …, Y. H. Sanejouand. 2000. Building-block approach for determining low-frequency normal modes of macromolecules. *Proteins.* 41:1–7.

19. Atilgan, A. R., S. R. Durell, …, I. Bahar. 2001. Anisotropy of fluctuation dynamics of proteins with an elastic network model. *Biophys. J.* 80:505–515.

20. Metropolis, N., A. W. Rosenbluth, …, E. Teller. 1953. Equation of state calculations by fast computing machines. *J. Chem. Phys.* 21:1087–1092.

21. Hill, T. L. 1987. An Introduction to Statistical Thermodynamics. Dover Publications, Mineola, NY.

22. Ben-Shaul, A., and W. M. Gelbart. 1994. Statistical thermodynamics of amphiphile self-assembly. *In* Micelles, Membranes, Microemulsions and Monolayers. W. M. Gelbart, A. Ben-Shaul, and D. Roux, editors. Springer, New York.

23. Tolar, P., J. Hanna, …, S. K. Pierce. 2009. The constant region of the membrane immunoglobulin mediates B cell-receptor clustering and signaling in response to membrane antigens. *Immunity.* 30:44–55.

24. Wu, Y., X. Jin, …, A. Ben-Shaul. 2010. Cooperativity between *trans* and *cis* interactions in cadherin-mediated junction formation. *Proc. Natl. Acad. Sci. USA.* 107:17592–17597.

25. Cavey, M., and T. Lecuit. 2009. Molecular bases of cell-cell junctions stability and dynamics. *Cold Spring Harb. Perspect. Biol.* 1:a002998.

26. Cebecauer, M., M. Spitaler, …, A. I. Magee. 2010. Signaling complexes and clusters: functional advantages and methodological hurdles. *J. Cell Sci.* 123:309–320.

27. Weikl, T. R., M. Asfaw, …, R. Lipowsky. 2009. Adhesion of membranes via receptor-ligand complexes: domain formation, binding cooperativity, and active processes. *Soft Matter.* 5:3213–3224.

28. Schmidt, D., T. Bihr, …, A. S. Smith. 2012. Coexistence of dilute and densely packed domains of ligand-receptor bonds in membrane adhesion. *EuroPhys. Lett.* 99:38003.

29. Sackmann, E. 2006. Thermo-elasticity and adhesion as regulators of cell membrane architecture and function. *J. Phys. Condens. Matter.* 18:R785–R825.

30. Perez, T. D., M. Tamada, …, W. J. Nelson. 2008. Immediate-early signaling induced by E-cadherin engagement and adhesion. *J. Biol. Chem.* 283:5014–5022.

31. Braun, J., J. R. Abney, and J. C. Owicki. 1984. How a gap junction maintains its structure. *Nature.* 310:316–318.

32. Bruinsma, R., M. Goulian, and P. Pincus. 1994. Self-assembly of membrane junctions. *Biophys. J.* 67:746–750.

33. Davis, S. J., and P. A. van der Merwe. 2006. The kinetic-segregation model: TCR triggering and beyond. *Nat. Immunol.* 7:803–809.

34. James, J. R., and R. D. Vale. 2012. Biophysical mechanism of T-cell receptor triggering in a reconstituted system. *Nature.* 487:64–69.

35. Hyman, A. A., and K. Simons. 2012. Cell biology. Beyond oil and water—phase transitions in cells. *Science.* 337:1047–1049.

36. Helfrich, W. 1978. Steric interaction of fluid membranes in multilayer systems. *Phys. Sci.* 33:305–315.

37. Helfrich, W. 1973. Elastic properties of lipid bilayers: theory and possible experiments. *Z. Naturforsch. C.* 28:693–703.

38. Simson, R., E. Wallraff, …, E. Sackmann. 1998. Membrane bending modulus and adhesion energy of wild-type and mutant cells of *Dictyostelium* lacking talin or cortexillins. *Biophys. J.* 74:514–522.